

Magnetic properties of small size-selected Co and CoPt clusters on Ni

L. Glaser,^{*} K. Chen, S. Fiedler, M. Wellhöfer, W. Wurth, and M. Martins[†]

University Hamburg, Luruper Chaussee 149, 22761 Hamburg, Germany

(Received 8 February 2012; revised manuscript received 6 July 2012; published 15 August 2012)

Size and stoichiometry-dependent magnetic properties of deposited Co and CoPt alloy clusters on a Ni/Cu(100) substrate have been investigated by use of x-ray magnetic circular dichroism spectroscopy. Using sum rules, spin and orbital moments were extracted from the spectra. Spin and orbital moments show a strong size-dependent effect with a tendency for an increase with cluster size, which is in contrast to observations for Co clusters on a Pt(111) surface. Addition of a Pt atom to a Co dimer leads to a doubling of the orbital moment. CoPt clusters show a strong increase in chemical reactivity towards oxidation. The resulting Co_nPtO_x clusters show a ratio of orbital to spin moment comparable to the pure clusters, however, with a strong suppression of the absolute orbital and spin moments.

DOI: [10.1103/PhysRevB.86.075435](https://doi.org/10.1103/PhysRevB.86.075435)

PACS number(s): 75.75.-c, 36.40.-c, 75.20.Hr, 78.70.Dm

I. INTRODUCTION

In common magnetic storage media the information is stored in small unequally sized magnetic grains. Storing bits with out-of-plane magnetized grains, instead of in-plane, led to a jump in storage density. Further increase can be achieved by scaling down the grain size for one bit and will soon require equally sized magnetic grains. The stability of information storage in the grains is related to the magnetic anisotropy energy (MAE), which has to be overcome in order to flip the magnetization. High MAE is essential for any material to qualify as building block for smaller grains. Promising hard magnetic materials are alloys of strong ferromagnets as Fe, Co, Ni with elements that show strong spin orbit coupling as Au or Pt. Experiments measuring MAE of Co atoms and clusters on Pt surfaces have shown extremely high values combined with large orbital magnetic moments for atoms, however, unfortunately with a monotoneous decrease for increasing average cluster sizes.^{1,2} Atoms and small clusters have proven to be ideal model systems to investigate magnetic properties, since these systems can be prepared and measured experimentally very accurately and are small enough for fully relativistic theoretical calculations, including hybridization and correlation effects. In particular, correlation effects are not negligible when the orbital magnetic moment is an important value, as in case of the MAE.

A few experimental studies on the magnetic properties of small, mass-selected clusters have been performed. The pioneering Stern-Gerlach type experiments on free cluster ions^{3,4} have shown a strong size dependence of the total magnetic moments. Recently, the first x-ray magnetic circular dichroism (XMCD) experiments of $3d$ metal cluster ions stored in a trap have been performed,^{5,6} showing, e.g., an antiferromagnetic coupling of the central Fe atom in a Fe_{13}^+ cluster. However, for possible applications the interaction with the surface is crucial and will strongly influence the magnetic properties of the clusters. This can be easily seen by comparing the XMCD results of Niemeyer *et al.*⁶ for free Fe clusters, with the corresponding results of Lau *et al.*^{7,8} for Fe clusters, deposited on thin, magnetized Ni films. For $3 \leq n \leq 9$ the magnetic moments of the free clusters show a rather smooth increase with cluster size up to $n = 6$. However, for the deposited clusters in particular, the orbital moments

show strong variations that completely differ from the free clusters, e.g., from $n = 5$ to $n = 6$ μ_ℓ increases by almost 60% for deposited clusters, which, for the free Fe clusters, μ_ℓ decreases slightly.

For tailoring, the magnetic properties of the deposited clusters, the size of the clusters, as well as the substrate are important parameters. A further possible variable, which has not been studied yet, is the composition dependence of the clusters, which will be the topic of this paper.

In order to investigate experimentally how magnetic moments of small, deposited Co and CoPt alloy clusters evolve with size and stoichiometric ratio, we performed XMCD measurements on deposited mass-selected clusters. Due to the chemical selectivity of XMCD, it is well suited to investigate dilute systems or single elements from alloys. Above that, XMCD as an integrating measurement allows us to investigate the average of an ensemble of several thousand equally prepared systems complementary to single-case investigations of STM studies.

II. EXPERIMENTS

The Co and CoPt alloy clusters were produced by ion sputtering⁹ using 30-keV Xe^+ ions from a high-purity $\text{Co}_{25}\text{Pt}_{75}$ target (99.9%). The positively charged cluster ions were collected and accelerated by an electrostatic lens system to a kinetic energy of 500 eV and mass separated with a dipole magnet, giving a resolution of $m/\Delta m \approx 50$. Production and mass separation of the clusters was carried out at a base pressure of 1×10^{-8} mbar. A more detailed description of the cluster source and its capabilities is given in Ref. 10. The clusters were deposited on 20-monolayer thin, out-of-plane magnetized Ni films prepared on a Cu(100) single crystal. To avoid fragmentation and implantation of clusters into the substrate surface during deposition, the clusters were decelerated down to a kinetic energy below 1 eV per cluster. In addition, a soft landing scheme¹¹ was used during cluster deposition, where ≈ 5 atomic layers of krypton were frozen onto the He-cooled sample. Soft landing into a rare gas buffer effectively suppresses cluster fragmentation during deposition.^{12,13} The krypton is desorbed by flash heating to ≈ 100 K leaving the clusters directly on the substrate's surface. The sample temperature was kept at ≈ 40 K to inhibit cluster

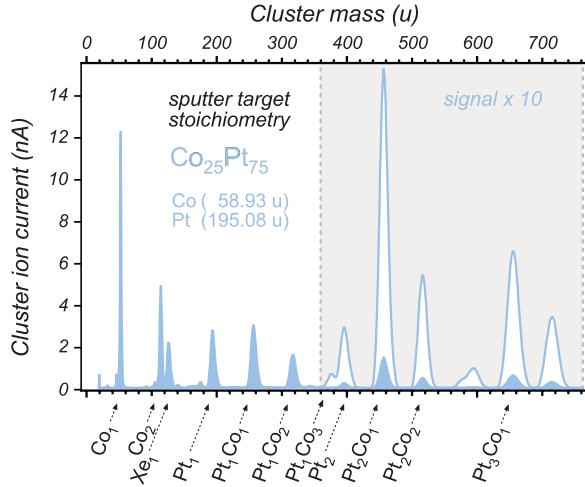


FIG. 1. (Color online) Mass spectrum of a $\text{Co}_{25}\text{Pt}_{75}$ sputter target (open graph: signal $\times 10$). The decrease of the pure Co and pure Pt clusters follow a normal exponential decay¹⁴ of cluster-ion-current intensity, while mixed clusters containing Pt and Co are more stable than pure Pt clusters.

diffusion during the measurement, while a low cluster coverage of 3% of a monolayer was chosen to avoid any cluster-cluster interaction and statistic agglomeration. As a measure for the x-ray absorption the total electron yield (TEY) was recorded. All cluster samples were prepared *in situ*, while measurements were carried out at a base pressure below $p < 2 \times 10^{-10}$ mbar. No traces of oxygen were observed in the residual gas analyzer.

The experiments were performed at beamline UE52-SGM at the BESSY II storage ring in Berlin. XMCD spectra of the deposited clusters were taken at the Co L edges in the photon energy range from 755 to 820 eV with counting times of 2×4 s per data point for each photon helicity. The substrate magnetization was measured at the Ni L edges in the photon energy range of 840 to 880 eV with counting times of 1 s per data point for each photon helicity. The beamline resolution was set to 100 meV, while the measuring geometry was such that the photons were incident normal to the sample surface. Hence, the photon helicity and the sample magnetization were oriented parallel or antiparallel, ensuring maximum contrast in the XMCD signal. For XMCD measurements the magnetization was kept constant, while the photon helicity was reversed.

A mass spectrum of CoPt clusters is given in Fig. 1. Co_nPt_m^+ clusters can be produced with up to six Pt atoms per cluster. Starting from Pt_2^+ the corresponding CoPt_m^+ with one additional Co atom gives always an almost 3 times larger cluster current. For the Co_2Pt_1^+ still an increase by a factor of 2 is found. Clusters of the type Co_3Pt_m have a mass slightly smaller than Pt_{m+1} clusters. In the mass spectrum these clusters are observed as a weak shoulder in front of the Pt_{m+1} peaks.

III. RESULTS AND DISCUSSION

XMCD spectra were recorded for Co atoms and cluster sizes $\text{Co}_{(n=2,3)}$, Co_1Pt_1 , and Co_2Pt_1 on Ni/Cu(100). For these cluster sizes the deposition time could be kept below 1 h for 3% of a monolayer coverage. In Fig. 2 the XMCD spectra for

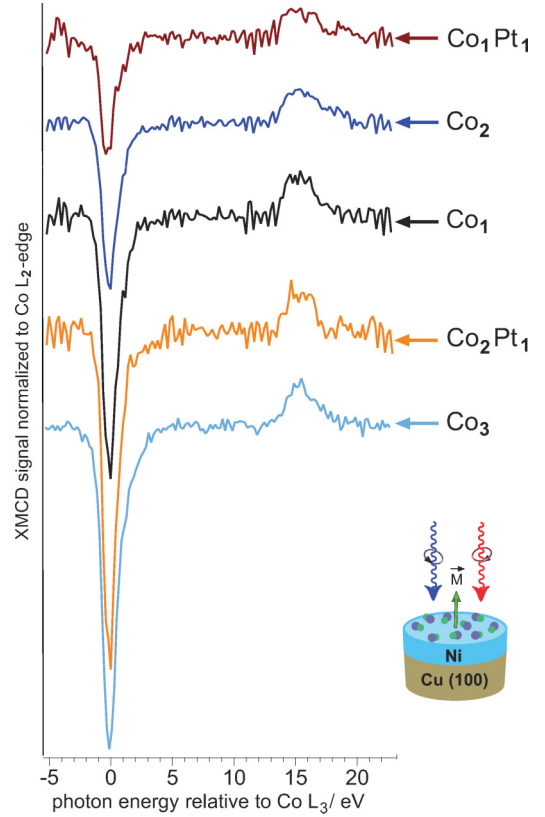


FIG. 2. (Color online) XMCD spectra of different Co_nPt_m clusters normalized to the L_2 signal deposited on an out-of-plane magnetized Ni/Cu(100) substrate. For a better comparison of the spectra the energy scale is given relative to the maximum XMCD signal at the Co L_3 edge.

these clusters are depicted. All spectra are normalized to the same intensity at the L_2 edge, so the L_3 XMCD signal is a measure for the ratio of the orbital to spin moment m_ℓ/m_s . For the different cluster sizes a strong, nonmonotonous variation of the XMCD signal is observed. From the graph, the strong influence of only one Pt atom on the magnetic properties of the Co clusters is obvious. The largest ratio is found for Co_2Pt_1 , whereas for Co_1Pt_1 the smallest m_ℓ/m_s is observed. For Co the separation of the L_3 and the L_2 contribution of the spectrum is possible, hence, allowing the straightforward application of sum rules.¹⁵ Because the number of d holes h_d for the different clusters is not known the results in this letter are presented as magnetic moments per d hole. Using sum rules, the absolute moments have been extracted from the XMCD spectra and are summarized in Table I. Again, by far the largest absolute spin and orbital moments are found for Co_2Pt_1 . Compared to the Co dimer, the orbital moment is increased by a factor of 2. By adding a Co atom instead of Pt to the Co dimer an increase in the ratio m_ℓ/m_s is also found; however, the spin moment is almost constant or even slightly reduced and the orbital moment is increased by only 50%. It should be noted that, for the Co dimer, the largest spin moment of the pure clusters is found in addition to the lowest orbital moment.

A different behavior is found for Co_1Pt_1 deposited on Ni/Cu(100). Here the ratio drops to a rather small value. The reason for this strong decrease can be found in an

TABLE I. Magnetic moments of Co and CoPt clusters on Ni/Cu(100) in comparison to different nanoparticles and thin films. There is a huge effect, when adding Pt to a Co dimer, the orbital moment doubles. The data for Co on Pt(111) is taken from¹ with $h_d = 2.40$. For comparison, the T_z for Co₁/Pt(111) is not taken into account. The error for the ratio is ± 0.03 and for the spin and orbital moment an error of $\pm 0.04\mu_B$ and $\pm 0.03\mu_B$ has been evaluated, respectively. For the nanoparticles also the substrate is given; aC is amorphous carbon.

Sample	m_l/m_s	$m_s/(\mu_B h_d)$	$m_l/(\mu_B h_d)$
Co ₁	0.30	0.51	0.15
Co ₂	0.20	0.57	0.12
Co ₃	0.37	0.55	0.20
Co ₂ Pt ₁	0.39	0.62	0.24
Co ₁ Pt ₁ + O	0.17	0.21	0.04
Co ₂ Pt ₁ + O	0.38	0.24	0.09
Co ₁ /Pt(111) ¹	0.61	0.75(5)	0.46
Co ₂ /Pt(111) ¹	—	—	0.32
Co (bulk)	0.10	0.55	0.05
Co _{7.5} nm/Ni/W(110) ^{19,20}	0.08	0.60	0.05
Co ₈ nm/Au(111) ²¹	0.14	0.56	0.08
CoPt ₃ nm aC ²²	0.09	0.73	0.07
CoPt (film) ²³	0.13	0.75	0.10
CoPt ₃ (film) ²⁴	0.19	0.71	0.06

enhanced chemical reactivity of the CoPt alloy clusters. The fine structure of the L₃ white line of the 3d transition metals is, in general, sensitive to the chemical environment, e.g., the oxidation state of the 3d metal. For the case of Cr clusters on a Ru(100) surface, this has been demonstrated by Lau *et al.*¹⁶ Thus, by monitoring the L₃-edge line shape for the deposited Co and CoPt clusters, the oxidation state of the sample can be probed throughout the time span of each XAS and XMCD measurement.

All pure Co_n clusters on Ni/Cu(100) were oxide free and showed no sign of oxidation or other degradation at any stage during the measurements. Even dosing >500 L oxygen on a Co₁ preparation does not change the x-ray absorption spectra. Annealing to 120 K in the presence of oxygen finally led to the oxidation of the deposited Co atoms. However, it proved hard to prepare Co₂Pt₁ oxide free and it was impossible to stabilize Co₁Pt₁ on the Ni/Cu(100) surface under the described UHV conditions. Comparing the XAS data of Co₁Pt₁ in Fig. 3 with spectra of oxide-free Co₁ and fully oxidized Co nanoparticles,¹⁷ one can estimate the degree of oxidation of the oxidized clusters. From this, $\approx 50\%$ oxidation can be deduced already at the first scan (15 min after cluster deposition), increasing to an average up to 65% oxidation within 3 h for the case of Co₁Pt₁. The presence of Pt on the Ni/Cu(100) substrate seems to have a strong catalytic effect on the oxidation process of the cobalt atoms, even at the low temperature of ≈ 40 K. This could be due to an increased electron density at the cobalt induced by the Pt via 3d-5d hybridization. This effect is weakened if one Pt atom hybridizes with two Co atoms, as in Co₂Pt₁, in which case the increased reactivity is still present, but oxidation occurs on a longer time scale, making XAS experiments on pure Co₂Pt₁ clusters possible. Nevertheless, this oxidation process allows

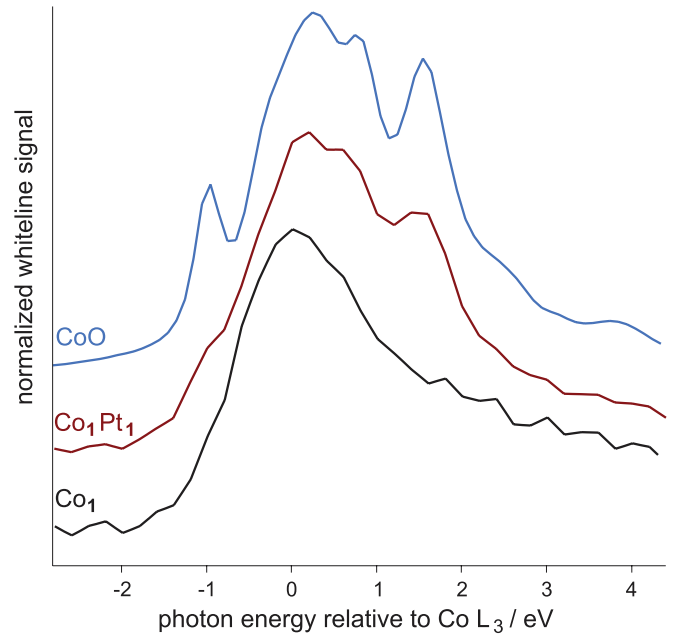


FIG. 3. (Color online) L₃ x-ray absorption spectra of deposited Co₁, Co₁Pt₁ clusters and CoO nanoparticles.¹⁷ The energy scale is given relative to the Co L₃ edge.

us to investigate also the magnetic properties of compound clusters of the type PtCo_nO_x.

Bulk CoO as an antiferromagnet usually does not show any XMCD signal. However, uncompensated Co spins in CoO have been observed in Fe/CoO/Ag(100) layer systems by Abrudan *et al.*,¹⁸ showing a weak circular dichroism signal. According to the smaller normalized L₃ dichroism intensity, they assume a much larger orbital moment of the electrons compared to the metallic Co case. In Table I, the magnetic moments for the oxidized clusters Co_nPt₁ + O are listed. Compared to the bulk values for Co and CoPt, the ratio of the oxidized clusters are enhanced; however, for the deposited clusters this increase is not caused by an enhanced orbital moment compared to Co_n and Co₂Pt. The absolute moments m_l and m_s both are strongly reduced by a factor of 2 to 3 and the large ratio is a result of the strongly quenched spin moment m_s . Both oxidized clusters show almost the same spin moment in the range from 0.21 to 0.24 μ_B . Thus, a noncollinear coupling of the Co atoms in Co₂PtO_x in line with the antiferromagnetism in CoO, reducing the effective moments, is unlikely as in CoPtO_x, only one Co atom is present and the strong reduction has to be a result of the hybridization of the Co 3d electrons with the Pt 5d and, in particular, oxygen valence electrons (Fig. 4).

Comparing the orbital to spin moment ratios of Co atoms on Ni with those of Co atoms on Pt(111)¹, the ratio more than triples from the Ni to the Pt substrate. For the Co dimer on Pt(111) the ratio decreases by $\approx 30\%$ to 0.32 compared to the atom, which is still a factor of 2.5 larger than the ratio for Co₂ on Ni/Cu(100). The ratio for Co₂Pt₁ on Ni/Cu(100) is roughly 30% smaller than for Co₂ on Pt(111). Thus, the single Pt atom can increase the ratio, but only to a smaller amount as compared with the Pt(111) surface. This effect might be

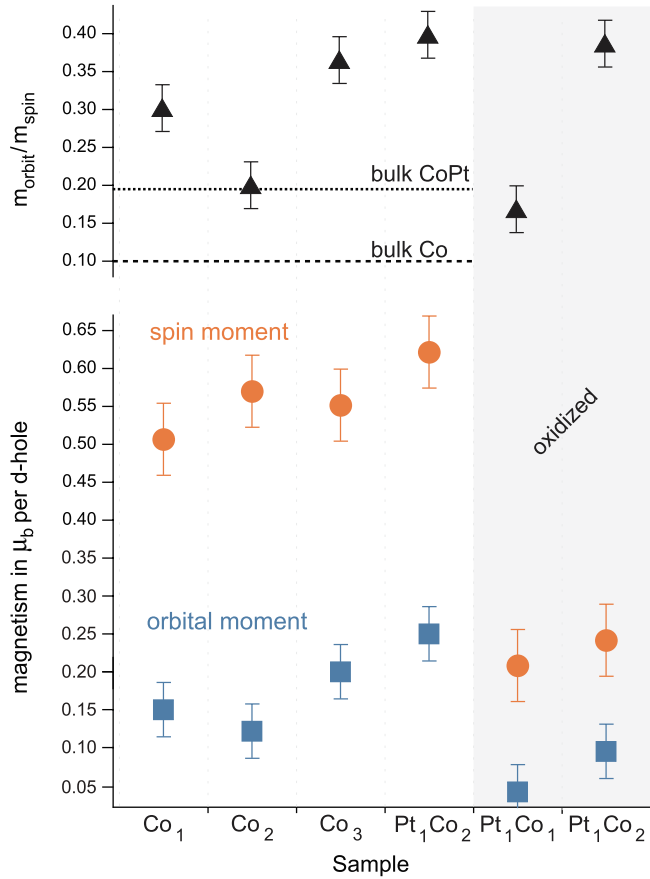


FIG. 4. (Color online) $\text{Co}_{1,2,3}$ and Co_2Pt_1 orbital (■) and spin (●) magnetic moments per $3d$ hole and their ratio (▲) compared to the bulk values of cobalt (dashed line)²⁶ and CoPt_3 (dotted line).²³

explained by the smaller number of Pt atoms taking part in the $3d$ - $5d$ hybridization with the Co dimer.

Please note that for the pure Co clusters there are differences in the size dependence on the different substrates. The measurements of Gambardella *et al.* of non-size-selected clusters on the Pt surface have shown a monotonous decrease of the orbital-to-spin-moment ratio with increasing cluster size, which is well reproduced by the calculations of Sipr *et al.*²⁵ However, for the Ni/Cu(100) substrate, the ratio decreases from Co_1 to Co_2 and is largest for Co_3 . It should also be noted that the experiments of Gambardella *et al.*¹ have been performed in a strong, external magnetic field to aligning the magnetic moments, whereas, in our case, the strong electronic interaction with the remanently magnetized Ni substrate leads to the magnetism of the clusters.

The absolute value of the spin moments m_s determined by the XMCD sum rules is influenced by the term T_z , which describes the magnetic spin dipole moment. In spherical geometry T_z is negligible and is typically assumed to be zero for sum-rule evaluation. For Fe, Co, and Ni bulk, thin-film systems^{27–30} and Co nanoparticles,^{19–21} all experimental data have so far supported this practice, but the influence of the strong spin orbit coupling Pt may lead to a nonvanishing component of T_z , e.g., for Co atoms on Pt(111), a T_z contribution in the order of 20% of the total moment has been evaluated.¹ Thus, depending on the geometry of the clusters

and its composition, the magnetic spin moments given in Table I might be influenced by T_z , in particular in Co_nPt clusters.

Spin and orbital moments found for the deposited clusters are rather low compared to the maximum value of $\mu_s = 1\mu_B/n_h$, which can be expected for a free atom and has been observed for the free Co_n^+ clusters with $n \geq 8$ by Peredkov *et al.*⁵ One reason might be a not fully saturated alignment of the magnetic moments. However, in this case, a more smooth size dependence of the magnetic moments, e.g., an increase of the magnetic moments with increasing cluster size, would be expected. Also the strong influence of a single Pt atom on the magnetic properties of the Co dimer can hardly be explained by unsaturated magnetic moments but is a clear sign of quantum-size effects. As can be seen from Table I also for a single Co atom on the Pt(111) surface a decreased spin moment of $0.75\mu_B/n_d$ is observed. Hence, we conclude that the reduced spin moment per d hole as compared to isolated atoms or clusters is a result of the strong hybridization of the Co states with the substrate bands.

It is interesting to compare the spin and orbital magnetic moments of the mass-selected Co and CoPt clusters with data of corresponding nanoparticles (NP) deposited on different surfaces. For Co clusters with ≈ 7.5 -nm diameter deposited on magnetized Ni films on W(110)^{19,20} $\mu_s = 0.60\mu_B$ have been measured. Similar experiments on ≈ 8 -nm Co nanoparticles in a strong, external magnetic field, however, deposited on a Au(111)²¹ surface, have shown effective spin moments of $0.56\mu_B$. Hence, the spin moments of the mass-selected clusters are slightly smaller than the nanoparticles moments. However, this is not the case for the orbital moments. On a Ni surface, the 7.5-nm nanoparticles have an orbital moment of $0.05\mu_B$, as in the bulk. For the 8.0-nm nanoparticles on the Au(111) surface, the orbital moments are enhanced by 60% to $\mu_\ell = 0.08\mu_B$. All orbital moments found in this work for the Co_n clusters on the Ni/Cu(100) surface are clearly above the nanoparticle values.

A similar behavior is found by adding Pt to Co nanoparticles as well as to the mass-selected clusters. For 3-nm CoPt nanoparticles embedded in amorphous carbon, an enhanced spin moment relative to the Co nanoparticles of $0.73\mu_B$ has been found by Tournus *et al.*²² One should mention here that the magnetic moments of the 3-nm CoPt nanoparticles depend also on the preparation. The spin moment is enhanced to $0.62\mu_B$ by adding a Pt atom to the Co_2 clusters, but the enhancement is clearly below that of the nanoparticles. The orbital moment of the 3-nm CoPt_3 nanoparticles ($\mu_\ell = 0.68\mu_B$) is between the Co nanoparticle value on different surfaces [$\mu_\ell = 0.5\mu_B$ on Ni/W(110) and $\mu_\ell = 0.8\mu_B$ on Au(111)]. For the orbital moment of the Co_2Pt clusters, similarly to the Co_n clusters and in contrast to the spin moments, a strongly increased moment of $0.24\mu_B$ is measured.

Thus, for the spin moments of the mass-selected cluster a similar trend as for the nanoparticles is found, e.g., an increase of the spin moment when Pt is added; however, the absolute value of the spin moments is slightly below the nanoparticle values. For the orbital moments the situation differs. Here the mass-selected clusters show strongly enhanced values, up to 4 times larger than the nanoparticle orbital moments. A reasonable explanation for the rather low spin moments of the deposited Co and CoPt clusters in comparison to the free

Co clusters⁵ is the interaction with the Ni/Cu(100) surface. As already a single Pt atom has a strong effect on the magnetic and also the chemical properties, the surface will have similar effects. An effect of the surface is found also for the Co nanoparticles, e.g., increasing the spin moment from $0.56 \mu_B$ for an Au(111) substrate to $0.60 \mu_B$ for a Ni/W(110) surface.

Here further studies should be performed, by depositing the clusters on other surfaces, e.g., thin magnetized Fe films or aligning them in an external magnetic field. Also sophisticated theoretical studies should be performed, which would be especially very helpful to estimate the effect of noncollinear magnetic moments. In particular, the influence of different surfaces on the properties of the clusters are of great relevance for possible applications, as the surface is one of the variables in tailoring the properties of clusters and nanoparticles.

IV. CONCLUSIONS

To summarize, we have shown in this experimental study on the magnetic properties of deposited alloy clusters the strong

influence of a single Pt atom on the magnetic and also chemical properties of small Co clusters. Adding a Pt atom to a Co dimer increases the magnetic moments strongly and, in particular, the orbital moment is increased by a factor of 2. Comparing the magnetic moments of Co and CoPt nanoparticles, the spin moments of the mass-selected clusters are slightly lower; however, the orbital moments are enhanced up to a factor of 4.

Whereas the pure Co clusters are stable against oxidation, Co_nPt clusters deposited on Ni/Cu(100) are easily oxidized, even under UHV conditions and at low temperatures. This oxidation results in a very strong decrease of the orbital and spin moments of the cluster by a factor of 2 to 3, however, showing still rather large values for the μ_ℓ -to- μ_s ratio.

ACKNOWLEDGMENTS

The work was performed within the framework of the SFB668 project A7. The help of the BESSY beamline staff is grateful acknowledged.

*Permanent address: DESY, Notkestraße 85, 22607 Hamburg, Germany.

†Corresponding author: michael.martins@desy.de

¹P. Gambardella, S. Rusponi, M. Veronese, S. S. Dhesi, S. Rusponi, M. Veronese, S. S. Dhesi, P. H. Dederichs, K. Kern, C. Carbone, and H. Brune, *Science* **300**, 1130 (2003).

²T. Balashov, T. Schuh, A. F. Takács, A. Ernst, S. Ostanin, J. Henk, I. Mertig, P. Bruno, T. Miyamachi, S. Suga, and W. Wulfhekel, *Phys. Rev. Lett.* **102**, 257203 (2009).

³W. A. de Heer, *Rev. Mod. Phys.* **65**, 611 (1993).

⁴I. M. Billas, A. Chatelain, and W. A. de Heer, *Science* **265**, 1682 (1994).

⁵S. Peredkov, M. Neeb, W. Eberhardt, J. Meyer, M. Tombers, H. Kampschulte, and G. Niedner-Schatteburg, *Phys. Rev. Lett.* **107**, 233401 (2011).

⁶M. Niemeyer, K. Hirsch, V. Zamudio-Bayer, A. Langenberg, M. Vogel, M. Kossick, C. Ebrecht, K. Egashira, A. Terasaki, T. Möller, B. v. Issendorff, and J. T. Lau, *Phys. Rev. Lett.* **108**, 057201 (2012).

⁷J. T. Lau, A. Föhlisch, R. Nietubyc, M. Reif, and W. Wurth, *Phys. Rev. Lett.* **89**, 057201 (2002).

⁸J. T. Lau, A. Föhlisch, M. Martins, R. Nietubyc, M. Reif, and W. Wurth, *New J. Phys.* **4**, 98 (2002).

⁹W. Hofer, *Top. Appl. Phys.* **64**, 15 (1991).

¹⁰J. Lau, A. Achleitner, H.-U. Ehrke, U. Langenbuch, M. Reif, and W. Wurth, *Rev. Sci. Instrum.* **76**, 063902 (2005).

¹¹J. Lau, H.-U. Ehrke, A. Achleitner, and W. Wurth, *Low Temp. Phys.* **29**, 223 (2003).

¹²H. Cheng and U. Landman, *Science* **260**, 1304 (1993).

¹³S. Fedrigo, W. Harbich, and J. Buttet, *Phys. Rev. B* **58**, 7428 (1998).

¹⁴C. Staudt, R. Heinrich, and A. Wucher, *Nucl. Instrum. Methods B* **164**, 677 (2000).

¹⁵W. L. O'Brien and B. P. Tonner, *Phys. Rev. B* **50**, 12672 (1994).

¹⁶J. Lau, A. Achleitner, and W. Wurth, *Surf. Sci.* **467**, 834 (2000).

¹⁷P. Imperia, L. Glaser, M. Martins, P. Andreazza, J. Penuelas, V. Alesandrovic, H. Weller, C. Andreazza-Vignolle, and W. Wurth, *Phys. Status Solidi A* **5**, 1047 (2008).

¹⁸R. Abrudan, J. Miguel, M. Bernien, C. Tieg, M. Piantek, J. Kirschner, and W. Kuch, *Phys. Rev. B* **77**, 014411 (2008).

¹⁹J. Bansmann, M. Getzlaff, A. Kleibert, F. Bulut, R. Gebhardt, and K. Meiwes-Broer, *Appl. Phys. A* **82**, 73 (2006).

²⁰A. Kleibert, J. Passig, K.-H. Meiwes-Broer, M. Getzlaff, and J. Bansmann, *J. Appl. Phys.* **101**, 114318 (2007).

²¹J. Bansmann, A. Kleibert, F. Bulut, M. Getzlaff, P. Imperia, C. Boeglin, and K.-H. Meiwes-Broer, *Eur. Phys. J. D* **45**, 521 (2007).

²²F. Tournus, A. Tamion, N. Blanc, A. Hannour, L. Bardotti, B. Prével, P. Ohresser, E. Bonet, T. Epicier, and V. Dupuis, *Phys. Rev. B* **77**, 144411 (2008).

²³W. Grange, I. Galanakis, M. Alouani, M. Maret, J.-P. Kappler, and A. Rogalev, *Phys. Rev. B* **62**, 1157 (2000).

²⁴W. Grange, M. Maret, J.-P. Kappler, J. Vogel, A. Fontaine, F. Petroff, G. Krill, A. Rogalev, J. Goulon, M. Finazzi, and N. B. Brookes, *Phys. Rev. B* **58**, 6298 (1998).

²⁵O. Šipr, S. Bornemann, J. Minár, S. Polesya, V. Popescu, A. Šimůnek, and H. Ebert, *J. Phys. C* **19**, 096203 (2007).

²⁶O. Šipr, J. Minár, S. Mankovsky, and H. Ebert, *Phys. Rev. B* **78**, 144403 (2008).

²⁷R. Wu, D. Wang, and A. J. Freeman, *Phys. Rev. Lett.* **71**, 3581 (1993).

²⁸R. Wu and A. J. Freeman, *Phys. Rev. Lett.* **73**, 1994 (1994).

²⁹W. L. O'Brien, B. P. Tonner, G. R. Harp, and S. S. P. Parkin, *J. Appl. Phys.* **76**, 6462 (1994).

³⁰C. T. Chen, Y. U. Idzerda, H.-J. Lin, N. V. Smith, G. Meigs, E. Chaban, G. H. Ho, E. Pellegrin, and F. Sette, *Phys. Rev. Lett.* **75**, 152 (1995).